Biogeosciences Discuss., doi:10.5194/bg-2017-109, 2017
Manuscript under review for journal Biogeosciences
Discussion started: 28 April 2017

The short-term combined effects of temperature and organic matter enrichment on permeable coral reef carbonate sediment metabolism and dissolution

Coulson A. Lantz[1], Kai G. Schulz[1], Laura Stoltenberg[1], Bradley D. Eyre[1]

[1]Centre for Coastal Biogeochemistry, School of Environment, Science, and Engineering, Military Road Southern Cross University Lismore 2480 NSW Australia

Correspondence to: Coulson A. Lantz (Coulsonlantz@gmail.com)

Biogeosciences Discuss., doi:10.5194/bg-2017-109, 2017
Manuscript under review for journal Biogeosciences
Discussion started: 28 April 2017

Abstract

Rates of gross primary production (GPP), respiration (R), and net calcification (G_{net}) in coral reef sediments are expected to change in response to global warming (and the consequent increase in sea surface temperature) and coastal eutrophication (and the subsequent increase in the concentration of organic matter (OM) being filtered by permeable coral reef carbonate sediments). To date, no studies have examined the combined effect of seawater warming and OM enrichment on coral reef carbonate sediment metabolism and dissolution. This study used 22-hour *in situ* benthic chamber incubations to examine the combined effect of temperature (T) and OM, in the form of coral mucus and phytodetritus, on GPP, R, and G_{net} in the permeable coral reef carbonate sediments of Heron Island lagoon, Australia. Compared to control incubations, both warming (+2.4 ºC) and OM increased R and GPP. Under warmed conditions, R was enhanced to a greater extent than GPP, resulting in a shift to net heterotrophy and net dissolution. Under both phytodetritus and coral mucus treatments, GPP was enhanced to a greater extent than R, resulting in a net increase in GPP/R and G_{net}. The combined effect of warming and OM enhanced R and GPP, but the net effect on GPP/R and G_{net} was not significantly different from control incubations. These findings show that a shift to net heterotrophy and dissolution due to short-term increases in seawater warming may be countered by a net increase GPP/R and G_{net} due to short-term increases in nutrient release from OM.

1. Introduction

Despite occupying only 7.5% of the seafloor, coastal marine sediments are responsible for a large fraction (55%) of global sediment organic matter oxidation (Middelburg et al., 1997). Of the coastal marine sediment environments, coral reef sediments are one of the most severely threatened by global climate change (Halpern et al., 2007). Rates of sediment autotrophic production (gross primary productivity; GPP) on coral reefs are generally greater than rates of heterotrophic metabolism (respiration; R) (GPP/R > 1), such that the sediments are generally a net source of oxygen (Atkinson, 2011). Similarly, rates of sediment calcification are generally greater than rates of sediment dissolution ($G_{net} > 0$) on most reefs under current ocean conditions, such that coral reef sediments on 24-hour diel timescales are net precipitating, resulting in the long-term burial of carbon in the form of calcium carbonate (Eyre et al., 2014; Andersson, 2015). This long-term production of calcium carbonate is an important component of reef formation and the creation of sandy cays (Atkinson, 2011). However, due to anthropogenically-mediated processes such as sea surface temperature (SST) warming (Levitus et al., 2000) and coastal eutrophication (Fabricius, 2005), coral reefs sediments may soon be subjected elevated SSTs and excess

Biogeosciences Discuss., doi:10.5194/bg-2017-109, 2017
Manuscript under review for journal Biogeosciences
Discussion started: 28 April 2017

concentrations of OM (Rabouille et al., 2001). This could ultimately impact the balance in GPP/R and G_{net} in the sediment and potentially reduce the long-term accumulation of carbonate material on coral reefs (Orlando and Yee, 2016).

Given the recent predictions of SST increases on coral reefs of between 1.2 to 3.2 ºC by the end of this century (IPCC, 2013), there are concerns that the net benthic metabolic balance in coral reef sediments may shift away from net production and net calcification to a state of net heterotrophy and net dissolution (Pandolfi et al., 2011). While several coral reef studies have examined the response in individual calcifying organisms to increased seawater temperature (T) (e.g., Johnson and Carpenter, 2012; Shaw et al., 2016), only one study (Trnovsky et al., 2016) has examined the response in the permeable coral reef carbonate sediments. The majority of warming studies on marine sediments have been performed *ex situ* in more pole-ward latitudes (temperate to arctic environments) over a wide range of temperatures (2 – 30 ºC) (e.g., Tait and Schiel, 2013; Hancke et al., 2014). The bacterial communities residing in marine sediments generally display a hyperbolic temperature-production relationship where GPP increases with T (~ + 32 % per 1 ºC increase) until an optimal rate is reached roughly +2 – 3 ºC above naturally observed seasonal maxima. This T-GPP relationship then declines at higher temperatures (+4 - 6 ºC) due to the deactivation of component reactions (Bernacchi et al., 2001). In arctic and temperate marine sediment communities, the increase in T can alter the balance between GPP and R, with an observed shift towards net heterotrophy (GPP/R < 1) (e.g., Arnosti et al., 1998; Hancke and Glud, 2004; Weston and Joye, 2005). Trnovsky et al. (2016) found that warming also decreased GPP/R in coral reef sediments and reduced G_{net} due to enhanced sediment dissolution.

Ultimately, the magnitude of potential shifts in coral reef sediment GPP/R and G_{net} under global warming scenarios will depend critically on the availability of organic matter (OM) substrate for remineralisation (Ferguson et al., 2003; Rabalais et al., 2009). A review of coral reef sediment studies has shown that carbonate sediment dissolution is strongly controlled by the extent of OM decomposition in the sediments (Andersson, 2015). Coral reefs are classically characterized as oligotrophic, relatively deficient in major inorganic nutrients (Koop et al., 2001). Despite this classification, the relatively high rates of GPP (1 to 3 mol C m^{-2} d^{-1}) for these ecosystems (Odum and Odum, 1955), are evidence of the tightly coupled nutrient cycling between autotrophs and heterotrophs. However, the balance in sediment metabolism on coral reefs may change in response to OM over-enrichment associated with eutrophication (Bell, 1992). Coral reefs affected by eutrophication (e.g., Hawaii (Grigg, 1995), Indonesia (Edinger et al., 1998), Jamaica (Mallela and Perry, 2007), Puerto Rico (Diaz-Ortega and Hernandez-Delgado, 2014)) all exhibit elevated concentrations of OM in the water column

Biogeosciences Discuss., doi:10.5194/bg-2017-109, 2017
Manuscript under review for journal Biogeosciences
Discussion started: 28 April 2017

(particulate OM: 10 – 50 µmol C L^{-1}) and above average rates of sedimentation (5 – 30 mg cm^{-2} d^{-1}). Elevated concentrations of OM and increased rates of terrestrially derived sedimentation on coral reefs can cause a decline in hard coral cover and a relative increase in macroalgal cover, resulting in an overall degradation of coral reef habitat (Fabricius, 2005).

Eutrophication can increase the amount of OM processed in coral reef sediments through several processes, two of which were simulated in this study; 1) through local phytoplankton blooms in the water column in response to the runoff of inorganic and organic nutrients and the eventual sediment deposition of dead phytoplankton (referred to herein as phytodetritus) (Furnas et al., 2005) and 2) the release of coral mucus into the reef water column as a stress response of scleractinian corals to increased sedimentation and the subsequent sediment deposition of this bacteria-rich protein matrix (Ducklow and Mitchell, 1979). The sediment deposition of OM provides labile carbon substrate (and associated nitrogen and phosphorous) for immediate consumption by autotrophic and heterotrophic bacterial communities.

Studies which have examined the effect of increased concentrations of OM, such as coral mucus (e.g., Wild et al., 2004a) or coral spawn and phytodetritus (e.g., Eyre et al., 2008), on coral reef sediment metabolism have shown a short-term increase in GPP/R, contrasting the results provided from short-term temperature studies on coral reef sediments, where GPP/R decreased (Trnovsky et al., 2016). Experimental additions of coral mucus from *Acropora* spp. on Heron Island, Australia (conducted only in the dark) induced a ~ 1.5-fold increase in R (Wild et al., 2004b) while additions of *Fungia* spp. mucus from a reef in Aqaba, Jordan (also conducted in the dark; Wild et al., 2005) showed a ~ 1.9-fold increase in R. OM associated with a mass coral spawning event (coral gametes and subsequent phytodetritus produced in the water column) on Heron Island, Australia caused a 2.5-fold increase in sediment R and a 4-fold increase in sediment GPP (Glud et al., 2008). Unlike the short-term response in GPP/R to T, sediment metabolism remained net-autotrophic during the spawning event at Heron Island, with GPP/R ratios rising as high as 2.5 – 3.0 (Glud et al., 2008), implying that nutrients recycled from OM stimulated GPP in excess of R (Eyre et al., 2008) on relatively short timescales (hours to days). However, studies which have examined the effect of excess OM on coral reef sediment metabolism over longer time scales (weeks to months) have shown that, ultimately, GPP/R eventually shifts to net heterotrophy (e.g., Andersson, 2015; Yeakel et al., 2015). This suggests that despite an initial OM-induced increase in GPP/R, the net long-term effect within reef sediments may be a preferentially heterotrophic recycling of nutrients released from organic matter degradation. Therefore, questions remain if a predicted temperature-driven shift to net heterotrophy will be exacerbated or mitigated by the presence of excess organic matter filtered by coral reef

Biogeosciences Discuss., doi:10.5194/bg-2017-109, 2017
Manuscript under review for journal Biogeosciences
Discussion started: 28 April 2017

sediments. There are, to date, no studies that have examined the effect of OM on coral reef sediment G_{net}. A short-term increase in GPP/R in response to OM implies that sediment G_{net} may be enhanced by excess concentrations of OM given that coral reef sediments generally exhibits a positive GPP/R-G_{net} relationship (Cyronak et al., 2016) whereas a long-term decrease in GPP/R may result in a decrease in sediment G_{net}.

Therefore, seawater warming and eutrophication will likely increase GPP and R in coral reef sediments, but, altogether, there is a lack of research demonstrating how these perturbations, specifically in combination, will affect the balance in coral reef sediment organic (GPP/R) and inorganic (G_{net}) metabolism. To meet these needs, this study performed incubations using benthic chambers placed *in situ* in a shallow coral reef sediment environment for a period of 24 hours. Phytodetritus and coral mucus were added to chamber seawater under ambient and increased SST (+2.4 ºC) conditions and the corresponding changes in GPP, R, and G_{net} were measured. We hypothesized that the short-term combined treatments of seawater warming and OM loading would enhance GPP and R in the sediment, but, given the previously shown short-term response in GPP/R and G_{net} to seawater warming (decrease in GPP/R and G_{net}) and net response to OM loading (decrease in GPP/R, G_{net} response unknown), there would be a net decrease in GPP/R and G_{net} relative to control treatments.

2. Methods

2.1 Study site

This study was conducted at Heron Island, Australia (23º 27'S, 151º 55'E) in November 2016. The island is situated near the Tropic of Capricorn, at the southern end of the Great Barrier Reef (GBR) and contains a ~ 9 ha island surrounded by a ~ 24 ha coral reef with an average hard coral cover of roughly 39% (Salmond et al. 2015). The study site was located on the leeward side of the reef flat, roughly 100 m from the island shore, in a sandy patch where water depth varies between ~ 0.1 – 2.7 m due to semi-diurnal tidal changes. The site was predominately covered in permeable $CaCO_3$ sediments (~ 63%) with interspersed patches of hard coral dominated by *Acropora* spp. (Roelfsema et al., 2002). The $CaCO_3$ sediment at this site has a ~ 2:1 ratio of aragonite: high magnesium calcite (Cyronak et al., 2013a). Sediment grain size: 12.1%. 2 mm, 30.5% between 1 and 2 mm, 27.3% between 500 mm and 1 mm, 14.1% between 250 mm and 500 mm, 11.2% between 125 mm and 250 mm, 4.2% between 63 mm and 125 mm, and 0.6%, 63 mm (Cyronak et al., 2013b).

2.2 Experimental design

Biogeosciences Discuss., doi:10.5194/bg-2017-109, 2017
Manuscript under review for journal Biogeosciences
Discussion started: 28 April 2017

A total of four 22-hour diel incubations were conducted during 5 - 12 Nov 2016 in advective benthic chambers. Benthic net primary production (NPP), gross primary productivity (GPP), respiration (R), and net calcification (G_{net}) were compared under ambient (~ 0.63 µmol C L^{-1}) and elevated concentrations of organic matter (OM) (additions of ~ 21.3 µmol C L^{-1} phytodetritus or ~ 23.6 µmol C L^{-1} coral mucus) at ~ 28.2 ºC and ~ 30.6 ºC in an orthogonal design. Eight chambers were used per incubation day, with each of the four OM-temperature combinations replicated in two randomly assigned chambers (Fig. 1). The first two incubations included two replicate chambers using phytodetritus crossed with temperature (6 and 7 Nov 2016) while the next two incubations included two replicate chambers using coral mucus crossed with temperature (9 and 11 Nov 2016). Incubations were started at sunset (18:00) and ended the following day at dusk (16:00). This allowed for a two-hour period (16:00 – 18:00) where chambers could be moved to a new area of sediment, closed, and heated to the desired temperature offset before beginning the next set of incubations.

2.3 Benthic chambers

Advective benthic chambers were constructed out of clear acrylic with a height of 33 cm and a diameter of 19 cm (Huettel and Gust, 1992). A motorized clear disc in the top of the chamber was programmed to spin at a rate of 40 revolutions per minute, which had previously been determined to induce an advection rate of ~ 43 L m^{-2} d^{-1} at the study site (Glud et al., 2008). Roughly 10 - 12 cm of the base of the chamber was inserted into the sediment such that a ~ 4 L water column of seawater was enclosed within the chamber (height ~ 15 cm) upon closing by the lid. The exact water volume varied within each chamber and was calculated for each incubation by multiplying known areal coverage by measured chamber height (at three positions above the sediment). Prior to closing the chambers, the tops were left open for ~ 1 hour to allow settlement of disturbed sediment. Chambers were then sealed ~ 1 hour prior to the beginning of each incubation to allow each temperature treatment chamber to reach the desired temperature offset. Following this, at the beginning of each incubation, selected chambers (four of the eight) were injected with OM (either coral mucus or phytodetritus).

2.4 Temperature manipulation

The international panel on climate change (IPCC) representative concentration pathway (RCP) 8.5 projects an average 2.2 - 2.7 ºC increase in SST (IPCC, 2013). A similar increase in temperature within the benthic chambers was achieved with 5W, silicone-heating pads (RS Australia) inserted inside of each of the four temperature treatment chambers (e.g., Trnovsky et al., 2016). These pads resided in the middle of the chamber water column and were powered by a 12 V battery on a surface support station tethered roughly 3 m away.

Biogeosciences Discuss., doi:10.5194/bg-2017-109, 2017
Manuscript under review for journal Biogeosciences
Discussion started: 28 April 2017

Temperature and light was measured in all eight chambers and in the water column using HOBO temperature loggers, which recorded temperature (ºC) and light (Lux) at an interval of fifteen minutes. Light intensity (Lux) was converted to µmol quanta of photosynthetic active radiation (PAR) m^{-2} s^{-1} using a conversion factor of 0.0185, derived from correlations with PAR measurements of a calibrated ECO-PAR (Wetlabs) sensor over a period of five days (R^2 = 0.89).

Heating pads increased temperature (T) within the chambers by 2.4 ± 0.5 ºC and maintained this offset on top of the natural diel temperature fluctuations measured in the control chambers (Table 1). As HOBO temperature loggers may record potentially higher than surrounding seawater temperatures due to internal heating of the transparent plastic casing (Bahr et al., 2016; Trnovsky et al., 2016), HOBO temperature data was corrected for precision (48-hour side-by-side logging of all nine loggers in an aquarium) and accuracy (deployment next to an *in situ* SeapHOx (Sea-Bird Electronics) for 48 hours). The conductivity sensor of the SeapHOx was used to record water column salinity for the duration of the experiment (7 days) at a sampling frequency of 30 minutes.

2.5 Organic matter manipulations

Phytodetritus (PD) was injected into treatment chambers to achieve a concentration increase by ~ 20 µmol C L^{-1}, a value analogous to mean conditions observed on degraded eutrophic coral reefs, where water column conditions can range from 10 to 50 µmol C L^{-1} (Fabricius et al., 2005, Diaz-Ortega and Hernandez-Delgado, 2014). Unfiltered seawater (6 L) was collected from the coastal ocean adjacent to the SCU laboratories (Lennox Head, NSW, Australia), containing naturally occurring assemblages of phytoplankton species common to the East Australian current. Collected seawater was stimulated with additions of 128 µmol L^{-1} NO_3^-, 8 µmol L^{-1} PO_4^{3-}, and 128 µmol L^{-1} H_4SiO_4 (buffered by additions of 256 µmol L-1 of HCl), and a solution of trace metals and vitamins ($F_{1/8}$; Guillard, 1975). Total amounts of nutrients were chosen to allow for a community production of up to 850 µmol C L^{-1} assuming a classical C: N: P Redfield ratio of 116:16:1 and a N:Si requirement of diatoms of 1. After a week of incubation at 150 µmol quanta of PAR m^{-2} s^{-1} at 20 ºC, the phytoplankton community was concentrated to 1/50th the original volume (0.12 L) via gentle (> -0.2 bar) vacuum filtration and rinsed with artificial seawater to remove residual concentrations of dissolved organic and inorganic nutrients. The resulting phytoplankton concentrate (measured at 8.5 µmol C L^{-1} and 0.9 µmol N L^{-1} of particulate organic carbon (POC) and nitrogen (PON), respectively; see section 2.6) was stored in the dark at 4.0 ºC until experimental use (6 days). At the beginning of an incubation, 10 ml of the dead phytoplankton concentrate, referred to as PD, was injected into each treatment chamber (~4 L volume), raising the

Biogeosciences Discuss., doi:10.5194/bg-2017-109, 2017
Manuscript under review for journal Biogeosciences
Discussion started: 28 April 2017

concentration of carbon and nitrogen by ~ 21.3 ± 1.0 µmol C L^{-1} and ~ 2.2 ± 0.8 µmol N L^{-1}, respectively (Table 1).

The amount of coral mucus (CM) added to the chambers was chosen to represent a reef-wide discharge of CM based on reported average mucus secretion rates for *Acropora* spp. (4.8 L mucus m^{-2} d^{-1}; Wild et al., 2004a), the dominant genus on the Heron Island reef flat. Mucus was collected from scattered branching coral fragments (*Acropora* spp.) using a non-destructive method whereby loose individual colonies naturally exposed to air during low tide were inverted so that gravity facilitated the pooling of secreted mucus through a cone filter into a large, 5 L beaker. This mucus was returned to the lab, particle filtered (5.0 µM) to remove the bulk of seawater, re-filtered to separate out particle carbonates, and stored in the dark at 4.0 ºC until experimental use (2 days). Ninety-four ml of mucus was injected into each treatment chamber to simulate the equivalent reported *Acropora* spp. mucus secretion rate (4.8 L mucus m^{-2} d^{-1}) for Heron Island given the average percent of this secreted mucus filtered by the sand (~ 70%; Wild et al., 2004a) and the benthic area enclosed by each chamber (0.028 m^2). Based on POC and PON concentrations (measured at 12.1 mmol C L^{-1} and 0.8 mmol N L^{-1}, respectively; see section 2.6) this represented an addition of ~ 23.6 ± 1.1 µmol C L^{-1} and 1.4 ± 0.4 µmol N L^{-1} (Table 1).

2.6 Sample collection and analysis

Seawater samples (120 ml total) were extracted from the top of each chamber via two two-port valves using two 60 ml syringes without headspace at ~12 hour intervals (sunset, dawn, and dusk) and returned to the lab for immediate analysis and/or preservation. 10 ml of unfiltered seawater from each chamber was analysed for dissolved oxygen (DO; mg L^{-1}) with a Hach HQ 30d meter and Luminescent DO (LDO) probe. Samples for seawater total alkalinity (A_T; µmol kg^{-1}) were filtered (0.45 µm; Chanson and Millero, 2007) and stored in 100 ml plastic, airtight bottles for immediate analysis (< 24 hours). Samples for dissolved inorganic carbon (DIC; µmol kg^{-1}) were also filtered (0.45 µM) into the bottom of 6 ml crimp vials (rubber butyl septum) with 5 ml overflow, and poisoned (6 µl of saturated $HgCl_2$; Dickson, 2007).

Seawater A_T was analysed using a potentiometric titration method (Dickson, 2007) on a Metrohm 888 Titrando automatic titrator using ~ 10 ml of seawater per sample. DIC was analysed on a Marianda AIRICA coupled to a Li-COR LI 7000 CO_2/H_2O Analyzer using ~ 1.6 ml of seawater per sample whereby four replicates of 400 µl were analysed for each sample and a best of three approach was used for each DIC calculation. A_T and DIC sample precision was estimated with replicate analyses conducted on every fifth sample (A_T SE = ± 1.7 µmol

Biogeosciences Discuss., doi:10.5194/bg-2017-109, 2017
Manuscript under review for journal Biogeosciences
Discussion started: 28 April 2017

211 kg^{-1}; DIC SE = ± 1.8 µmol kg^{-1}). Measurements were corrected against certified reference material (CRM;
212 Batch 155) from the Scripps Institute of Oceanography (A_T SE = ± 2.2 µmol kg^{-1}; DIC SE = ± 1.3 µmol kg^{-1}).
213 Parameters for the seawater carbonate system (Ω_{ar}, pH_T (total scale)) were calculated from measured A_T, DIC,
214 temperature, and salinity using the R package seacarb (Lavigne and Gattuso, 2013) with K_1 and K_2 constants
215 applied from Mehrbach et al. (1973) and refit by Dickson and Millero (1987). Because changes in A_T could be
216 due to processes other than the precipitation and dissolution of carbonates (e.g., sulfate reduction associated
217 with organic matter additions), fluxes in DIC were corrected for assumed A_T fluxes due to calcium carbonate
218 precipitation/dissolution (0.5 moles CO_2: 1 mole A_T) and compared against fluxes in O_2, with an expected 1:1
219 molar flux ratio (DIC_{org} : O_2).

220 Prior to chamber additions subsamples (1 ml, n = 3) were taken from the concentrated PD culture, CM, and the
221 water column and analysed for particulate organic carbon (POC) and nitrogen (PON). These subsamples were
222 filtered on pre-combusted 25mm GF/F filters, dried at 60 ºC, fumed with 12 M HCl to dissolve any particulate
223 carbonates on the filter, and wrapped in pre-combusted tin capsules. These capsules were analysed for carbon
224 (C) and nitrogen (N) using an elemental analyser (Thermo Flash ES) coupled to an isotope ratio mass
225 spectrometer (Thermo Delta V PLUS) via a Thermo Conflo V (see Eyre et al. 2016, for details).

226 **2.7 Calculating sediment metabolism**

227 Benthic metabolism (NPP, GPP, R, G_{net}) in each chamber was estimated based on the flux of measured solutes
228 (DO, and A_T, respectively). For flux calculations, DO was converted from mg L^{-1} to mmol L^{-1}. A_T and DIC were
229 converted from µmol kg^{-1} to mmol L^{-1} using calculated temperature and salinity dependent seawater density.
230 The solute flux equation (Glud et al., 2008) was as follows:

231 $$Equation 1 : F = \frac{\Delta S \times v}{A \times \Delta t}$$

232 Where F (mmol m^{-2} hr^{-1}) is the net flux in solute, ΔS (mmol L^{-1}) is the change in solute concentration, v (L) is
233 the chamber volume, A (m^2) is the area of sediment enclosed by the chamber, and Δt(hours) is the time elapsed
234 between seawater samplings. Rates of sediment net primary production (NPP), gross primary production (GPP),
235 and respiration (R) were calculated from O_2 fluxes (mmol O_2 m^{-2} hr^{-1}), and rates of net sediment calcification
236 (G_{net}) were calculated from A_T fluxes (mmol $CaCO_3$ m^{-2} hr^{-1}) (Table 2).

237 To determine the numerical relationship between a 10 ºC change in temperature and GPP and R, Q_{10} values
238 were estimated for temperature treatments according to the following equation:

Biogeosciences Discuss., doi:10.5194/bg-2017-109, 2017
Manuscript under review for journal Biogeosciences
Discussion started: 28 April 2017

$$Equation2: Q_{10} = \left(\frac{M2}{M1}\right)^{\left(\frac{10}{T_2 - T_1}\right)}$$

where *M1* is the metabolic rate (GPP or R) at temperature T_1 (control) and *M2* is the metabolic rate (GPP or R, respectively) at temperature T_2 (warming treatment), with $T_1 < T_2$.

2.8 Statistical analyses

Results are displayed as the mean ± standard error (SE). Data was organized as the 22-hour average (diel) of day and night values and was pooled together within each T, OM, and T + OM treatment. All statistical analyses were performed with the SPSS statistics software (SPSS Inc. Version 22.0) running in a Windows PC environment, and the assumptions of normality and equality of variance were evaluated with graphical analyses of the residuals. To test for the effect of each treatment (T, PD, and CM) on respiration, photosynthesis, and calcification, measured 22-hour R, NPP, GPP, and G_{net} were analysed using a repeated-measures three-way analysis of variance (ANOVA). In this model, temperature and OM (PD and CM) were fixed effects, the within-subject factor was time (days), and replicate chambers were a nested effect. To compare the significance of temperature and OM between and within treatment chambers, a one-way ANOVA model was used in which chamber was the fixed effect and average seawater temperatures (ºC) and POC and PON concentrations, respectively, were treated as the response variable. In these analyses, Bonferroni post-hoc test were used to conduct pair-wise comparisons between treatments.

The variation in NPP, GPP, R, and G_{net} provided the opportunity to explore the relationship between net organic and inorganic metabolism across all treatments. A Pearson correlation was used to test for an association between sediment G_{net}, NPP, GPP, R, and GPP/R. Where each of these pairwise correlations were statistically significant, Model I regression techniques were used to fit a linear relationship for the purpose of predicting inorganic metabolism (G_{net}) from organic metabolism (NPP, GPP, R, GPP/R).

3. Results

3.1 Measured seawater chemistry and sediment metabolism in control chambers

Temperature measured in the water column throughout the experiment (27.6 ± 1.3 ºC) exhibited typical diel changes and was slightly cooler relative to the average temperature inside control chambers (-0.8 ± 0.5 ºC) (Fig. 2). Mean water column salinity throughout the experiment was 35.8 ± 0.1. Over the course of each diel incubation period, changes in water chemistry (Fig. 3) were driven by benthic metabolism. Control (C)

Biogeosciences Discuss., doi:10.5194/bg-2017-109, 2017
Manuscript under review for journal Biogeosciences
Discussion started: 28 April 2017

chambers, pooled between all four incubations (n = 9), had an R of -1.3 ± 0.5 mmol O_2 m^{-2} hr^{-1} and an NPP of 1.9 ± 0.3 mmol O_2 m^{-2} hr^{-1}, yielding a GPP of 3.2 ± 0.6 mmol O_2 m^{-2} hr^{-1} and a GPP/R of 1.31 ± 0.12. C chambers were net dissolving at night (-0.9 ± 0.2 mmol $CaCO_3$ m^{-2} hr^{-1}) and net calcifying during the day (1.3 ± 0.2 mmol $CaCO_3$ m^{-2} hr^{-1}). Overall, 24-hour diel G_{net} ($F_{1,31}$ = 122.82, $p < 0.05$) was net calcifying (0.2 ± 0.1 mmol $CaCO_3$ m^{-2} hr^{-1}). Mean particulate organic carbon (POC) and nitrogen (PON) concentrations in the four C chambers was 0.63 ± 0.1 µg C L^{-1} and 0.12 ± 0.1 µg N L^{-1}, respectively.

3.2 The effects of temperature on sediment metabolism

Mean seawater temperature in the C and temperature (T) treatments during the four incubation periods was 28.2 ± 1.1 ºC and 30.6 ± 1.2 ºC, respectively (Table 1). Temperature differed between C and T treatments ($F_{1,31}$ = 384.38, $p < 0.05$), but there was no significant difference between replicate chambers within each treatment ($F_{1,31}$ =0.76, p = 0.768). Temperature in all eight chambers exhibited typical diel changes throughout all four incubation periods, driven by sunlight and tidal changes in water depth (Fig. 2). Treatment chambers followed the same natural diel change measured in control chambers and maintained an average +2.4 ± 0.5 ºC offset over the course of the study (Table 1).

Within the T treatments there was no significant difference in estimated metabolic rates between all four incubations ($F_{1,31}$ =1.2, p = 0.238), so rates were pooled. During the fourth incubation, one T treatment was lost due to a broken heater and this chamber was treated as a third control replicate. Seawater warming increased R to -3.5 ± 0.4 mmol O_2 m^{-2} hr^{-1} ($F_{1,31}$ = 260.38, $p < 0.05$) (Table 3), NPP to 2.9 ± 0.4 mmol O_2 m^{-2} hr^{-1} ($F_{1,31}$ = 192.17, $p < 0.05$), and GPP to 6.4 ± 0.5 mmol O_2 m^{-2} hr^{-1} ($F_{1,31}$ = 160.61, $p < 0.05$) (Fig. 4). Overall, warming decreased GPP/R to 0.93 ± 0.05 ($F_{1,31}$ = 79.02, $p < 0.05$), indicating a shift from net autotrophy to net heterotrophy (Fig. 5). Mean calculated Q_{10} values, averaged across T treatments from all four incubations, were 10.7 ± 3.1 for R and 7.3 ± 1.2 for GPP. Warmed chambers were net dissolving at night (-1.9 ± 0.2 mmol $CaCO_3$ m^{-2} hr^{-1}) and net calcifying during the day (1.7 ± 0.2 mmol $CaCO_3$ m^{-2} hr^{-1}). Overall, warming decreased G_{net} to -0.2 ± 0.1 mmol $CaCO_3$ m^{-2} hr^{-1} ($F_{1, 31}$ = 122.82, $p < 0.05$) (Fig. 6), indicating a shift to net dissolution.

3.3 The effects of organic matter on sediment metabolism

Mean POC and PON concentrations in the four phytodetritus (PD) treatment chambers was 21.7 ± 1.0 µg C L^{-1} and 2.3 ± 0.8 µg N L^{-1}, respectively (POC:PON ~ 9:1) (Table 1). During the PD treatment incubations, there was no significant difference in metabolic rates between incubations ($F_{1,15}$ = 0.32, p = 0.299), so estimated metabolic rates were pooled within the PD-only treatments. PD increased R to -2.6 ± 0.5 mmol O_2 m^{-2} hr^{-1} ($F_{1,15}$

Biogeosciences Discuss., doi:10.5194/bg-2017-109, 2017
Manuscript under review for journal Biogeosciences
Discussion started: 28 April 2017

= 16.77, $p < 0.05$) and increased NPP to 5.3 ± 0.5 mmol O_2 m^{-2} hr^{-1} ($F_{1,15}$ = 245.86, $p < 0.05$), thereby increasing GPP to 7.9 ± 0.4 mmol O_2 m^{-2} hr^{-1} ($F_{1,15}$ = 212.64, $p < 0.05$) and increasing GPP/R to 1.54 ± 0.11 ($F_{1,15}$ = 13.92, $p < 0.05$). Chambers treated with PD were net dissolving at night (-1.5 ± 0.2 mmol $CaCO_3$ m^{-2} hr^{-1}) and net calcifying during the day (2.8 ± 0.3 mmol $CaCO_3$ m^{-2} hr^{-1}). Overall, PD increased G_{net} to 0.6 ± 0.2 mmol $CaCO_3$ m^{-2} hr^{-1} ($F_{1,15}$ = 134.27, $p < 0.001$).

Mean POC and PON concentrations in the four coral mucus (CM) treatment chambers was 24.2 ± 1.1 µg C L^{-1} and 1.5 ± 0.4 µg N L^{-1}, respectively (POC:PON ratio ~ 16:1). During CM incubations, there was no significant difference in metabolic rates between incubations ($F_{1,15}$ =0.42, $p = 0.448$), so estimated metabolic rates were pooled together within CM-only treatments. CM increased R to -2.0 ± 0.4 mmol O_2 m^{-2} hr^{-1} ($F_{1,15}$ = 7.34, $p < 0.05$) and increased NPP to 4.4 ± 0.5 mmol O_2 m^{-2} hr^{-1} ($F_{1,15}$ = 134.51, $p < 0.05$), thereby increasing to 6.4 ± 0.6 mmol O_2 m^{-2} hr^{-1} GPP ($F_{1,15}$ = 99.24, $p < 0.05$) and increasing GPP/R to 1.61 ± 0.2 ($F_{1,15}$ = 34.17, $p < 0.05$). Chambers treated with CM were net dissolving at night (-1.3 ± 0.2 mmol $CaCO_3$ m^{-2} hr^{-1}) and net calcifying during the day (2.4 ± 0.3 mmol $CaCO_3$ m^{-2} hr^{-1}). Overall, CM increased G_{net} to 0.5 ± 0.2 mmol $CaCO_3$ m^{-2} hr^{-1} ($F_{2,22}$ = 100.61, $p < 0.05$).

3.4 The combined effects of temperature and organic matter on sediment metabolism

In the first two incubations (T + PD), there was no significant difference in metabolic rates between days ($F_{1,15}$ =1.23, $p = 0.135$), so estimated metabolic rates were pooled together within the T + PD treatments. T + PD increased R to -3.1 ± 0.5 mmol O_2 m^{-2} hr^{-1} ($F_{1,15}$ =46.4 $p < 0.001$), increased NPP to 4.7 ± 0.5 mmol O_2 m^{-2} hr^{-1} ($F_{1,15}$ =16.31, $p < 0.05$), and increased GPP to 7.8 ± 0.5 mmol O_2 m^{-2} hr^{-1} ($F_{1,15}$ =8.81, $p < 0.05$). GPP/R in T + PD treatments was 1.27 ± 0.18 (PD+T), a change that was not significantly different from control chambers ($F_{1,15}$ =2.75, $p = 0.122$). Chambers treated with T + PD were net dissolving at night (-1.9 ± 0.2 mmol $CaCO_3$ m^{-2} hr^{-1}) and net calcifying during the day (2.6 ± 0.3 mmol $CaCO_3$ m^{-2} hr^{-1}). Overall, 22-hour diel G_{net} in T + PD treatments was 0.3 ± 0.2 mmol $CaCO_3$ m^{-2} hr^{-1}, a change which was not significantly different from control chambers ($F_{1,15}$ =0.70, $p = 0.417$).

In the two last incubations (T + CM), there was no significant difference in metabolic rates between days ($F_{1,15}$ =1.73, $p = 0.110$), so estimated metabolic rates were pooled together within the combined T + CM treatments. T + CM and increased R to -2.9 ± 0.4 mmol O_2 m^{-2} hr^{-1} ($F_{1,15}$ =7.75, $p < 0.05$), increased NPP to 4.6 ± 0.5 mmol O_2 m^{-2} hr^{-1} ($F_{1,15}$ =17.19, $p < 0.05$), and increased GPP to 7.5 ± 0.5 mmol O_2 m^{-2} hr^{-1} ($F_{1,15}$ =26.77, $p < 0.05$). GPP/R in T + CM treatments was 1.21 ± 0.13, a change which was not significantly different from control chambers

Biogeosciences Discuss., doi:10.5194/bg-2017-109, 2017
Manuscript under review for journal Biogeosciences
Discussion started: 28 April 2017

($F_{1,15}$ =3.79, p = 0.075). T + CM chambers were net dissolving at night (-1.8 ± 0.3 mmol $CaCO_3$ m^{-2} hr^{-1}) and net calcifying during the day (2.4 ± 0.4 mmol $CaCO_3$ m^{-2} hr^{-1}). Overall, 22-hour diel G_{net} in T + CM treatments was 0.2 ± 0.2 mmol $CaCO_3$ m^{-2} hr^{-1}, a change which was not significantly different from control chambers ($F_{1,15}$ =0.87, p = 0.368).

Measured R in all chambers under all treatments was not significantly correlated with NPP (r = 0.53, df = 31, p > 0.05). However, in the C chambers, R was significantly correlated with NPP (r = 0.81, df = 31, p < 0.05). $CaCO_3$ precipitation during the day was positively correlated with NPP (r = 0.81, df = 31, p < 0.05; slope = 0.22 ± 0.08) while dissolution at night was positively correlated with R (r = 0.83, df = 31, p < 0.05; slope = 0.45 ± 0.04). Average diel G_{net} was positively correlated with GPP/R (r = 0.83, df = 31, p < 0.05; slope = 0.70 ± 0.05). The DIC_{org}:O_2 quotient for all treatments was 0.94 ± 0.09 on average and did not significantly differ from 1 (p < 0.05; Fig. 7), suggesting that sulfate reduction did not significantly contribute to the A_T fluxes.

4. Discussion

4.1 The response in coral reef sediment metabolism to seawater warming

In our experiment, seawater warming (+2.4 ± 0.5 ºC) was within the projection of the IPCC RCP 8.5 (+2.2 – 2.7 ºC). Under this elevated seawater temperature (T), R increased to a greater extent than GPP, shifting the sediments to net heterotrophy (GPP/R = 0.93) over the 22-hour incubation period (Fig. 8). Whereas NPP and R were significantly correlated in control chambers (p < 0.05), they were not significantly correlated in the warming treatments (p = 0.136), evidence that warming decoupled the balance in autotrophic: heterotrophic metabolism (Fig. 8). The decrease of GPP/R due to warming can be explained by the relatively lower measured Q_{10} value for GPP (7.3 ± 1.2) compared to R (10.7 ± 3.1). These results agree with other studies showing that seawater warming preferentially enhances R to a greater degree than GPP in marine sediments (Hancke and Glud, 2004; Weston and Joye, 2005; Tait and Schiel, 2013). The decline in GPP/R in response to warmer seawater temperature may be a product of the differential ranges in activation energies for GPP and R (Yvon-Durocher et al., 2010), where R exhibits a stronger and more rapid physiological acclimation to warming compared to GPP during short-term temperature variations (Wiencke et al., 1993; Robinson, 2000).

The observed 29% decrease in GPP/R in response to warming lead to a net 109% decrease in G_{net} (relative to control chambers), resulting in a transition to net sediment dissolution over the 22-hour incubation period (Fig. 8). This decrease in G_{net} was most likely due to a respiration-driven increase in porewater pCO_2 (e.g., Cyronak et al., 2013a), thereby decreasing the mean aragonite saturation state in the water column (mean Ω_{arg} = -0.7 relative

Biogeosciences Discuss., doi:10.5194/bg-2017-109, 2017
Manuscript under review for journal Biogeosciences
Discussion started: 28 April 2017

to control chambers) and porewater (where sediment dissolution occurred). While increasing T increases Ω_{arg} geochemically, the biologically driven changes in Ω_{arg} were most likely the dominant effect on the measured enhanced dissolution of the sediment given that a 2.4 ºC increase in temperature would only increase Ω_{arg} roughly 0.058 units.

Together, our results show that the warming of seawater by 2.4 ºC will decrease GPP/R 0.38 units and G_{net} 0.2 mmol $CaCO_3$ m^{-2} hr^{-1} in the permeable calcium carbonate sediments at this study site on Heron Island. The decline in the GPP/R in response to warming implies that a greater fraction of the carbon fixed by autotrophs was remineralised by heterotrophic bacteria and released as CO_2, thus compromising the capacity of coral reef permeable carbonate sediments to remain net autotrophic at an elevated seawater T. While a transition to net sediment dissolution under warmer conditions would consume CO_2, potentially alleviating some of the CO_2 release caused by a transition to net heterotrophy, a comparison of the rates measured in this study show the net effect would still result in a production of CO_2. Under the warmed conditions in this study, organic metabolism released ~ 5.28 mmol CO_2 m^{-2} d^{-1} while inorganic metabolism consumed ~ 1.44 mmol CO_2 m^{-2} d^{-1}, which resulted in a net production of 3.84 mmol CO_2 m^{-2} d^{-1} in the chambers.

Where the decline in marine sediment GPP/R in response to seawater warming has been previously reported in several studies (e.g., Woodwell et al., 1998; Hancke and Glud, 2004; Weston and Joye, 2005; Lopez-Urrutia and Moran, 2007), the decline in G_{net} has only been reported once (Trnovsky et al., 2016). It is important to note that these results should not be extrapolated beyond 2100, where SST continues above +2.4 ºC. The T increase simulated in this study (+2.4 ºC) was within the optimal temperature range (30.6 ºC) of previously reported temperature-metabolism hyperbolic relationships in marine sediments (Yvon-Durocher et al., 2010). Given that these hyperbolic relationships show that further increases in temperature (+3 - 5 ºC) can have an opposite effect on sediment metabolism (net decrease in GPP and R; Weston and Joye, 2005), we cannot conclude the results obtained here would scale linearly beyond ca. 2100.

4.2 The response in coral reef sediment metabolism to organic matter enrichment

Increased concentrations of organic matter (OM), analogous to eutrophic conditions on degraded coral reefs, enhanced both GPP and R in the sediment and likely released nitrogen and phosphorus via organic matter degradation (ΔGPP/R +0.27 relative to control chambers). These results agree with prior work, where increased concentrations of OM were quickly aerobically degraded by bacteria (within minutes - see Maher et al., 2013; to hours - see Ferrier-Pages et al., 2000) and enhanced GPP more than R (Glud et al., 2008; Eyre et al., 2008).

Biogeosciences Discuss., doi:10.5194/bg-2017-109, 2017
Manuscript under review for journal Biogeosciences
Discussion started: 28 April 2017

While some of this OM was likely degraded in the water column, previous experiments (e.g., Wild et al., 2004b) have shown that the high permeability of carbonate sediments permits the transport of OM into the upper centimetres (1 - 4 cm) of the sand, where bacterial degradation rates can exceed those of the water column by a factor of 10-12 (Moriarty, 1985; Wilkinson, 1987). Measured changes in GPP and R in response to elevated concentrations of OM in this study are therefore most likely a product of changes in metabolism in the bacterial communities residing in the upper layers of the sediment.

Phytodetritus (PD) and coral mucus (CM) enhanced respiration 1.1- and 0.6-fold, respectively, which was a less pronounced increase in R than the 1.5-fold increase observed by Wild et al. (2004b) using the same *Acropora* spp. mucus at Heron Island. However this discrepancy may be due to the fact their study used almost three times more CM (~ 280 ml) per treatment than this study (94 ml). An increase in GPP/R to 1.7 one day following the deposition of coral spawning material at the same study site (Glud et al., 2008), was similar to the average increase in GPP/R to 1.6 observed under increased OM concentrations in this study. PD enhanced GPP and R to a greater degree than CM, which may be explained by the different concentration of nitrogen in each source of OM. Particulate organic carbon additions differed by less than 10% between PD and CM treatments, whereas particulate organic nitrogen addition (N) was almost twice as high in the PD compared to the mucus CM, as indicated by the differing POC:PON ratio for PD (9:1) and CM (16:1). In general, bacterial communities responsible for the cycling of nutrients in sediments are thought to be nitrogen limited (Eyre et al., 2013). Given the relatively short timescale (24 hours) in which the response in sediment metabolism to OM was measured, we reason that the PD was more rapidly mineralized than CM due to a higher N content in the added PD (Oakes et al., 2011).

To our knowledge, this is the first experiment to examine the short-term relationship between OM degradation and G_{net} in coral reef sediments. Our results show that increased concentrations of PD and CM both enhanced G_{net} within the first 22 hours. Most likely the increase in G_{net} was a product of the same biogeochemical mechanism influencing G_{net} under seawater warming, whereby changes in GPP/R modify porewater pCO_2 and Ω_{arg}. In the case of OM, a preferential enhancement of GPP over R resulted in an increase in Ω_{arg} (mean Ω_{arg} = +0.6 relative to control chambers) and subsequent increase in G_{net} (net precipitation) (+1.4 mmol $CaCO_3$ m^{-2} hr^{-1} relative to control chambers). While the results presented here are the first to report a positive OM-G_{net} relationship specifically in permeable calcium carbonate sediments, a similar response has also been observed at the coral reef ecosystem level (Yeakel et al., 2015), where increased offshore productivity in the Sargasso Sea over the course of several months lead to an increase in community G_{net} on the adjacent Bermuda coral reef flat.

Biogeosciences Discuss., doi:10.5194/bg-2017-109, 2017
Manuscript under review for journal Biogeosciences
Discussion started: 28 April 2017

412 Interestingly, this increase in G_{net} in Bermuda coincided with a period of net heterotrophy on the reef. The
413 difference in the G_{net} – GPP/R relationship between the data in this study (OM increased GPP/R and increased
414 G_{net}) and those in Yeakel et al. (2015) (OM decreased GPP/R and increased G_{net}) may be a result of the
415 timescale of observation. This implies that, should elevated concentrations of OM persist for an extended period
416 of time (weeks to months), the immediate preferentially phototrophically-mediated recycling of nutrients, and
417 associated increased GPP/R and G_{net} in coral reef sediments, may eventually shift to net heterotrophy despite the
418 ability to maintain a positive G_{net}.

419 **4.3 The response in coral reef sediment metabolism to a combination of seawater warming and organic**
420 **matter enrichment**

421 The combination of seawater warming and increased concentrations of OM, for both PD and CM, exhibited an
422 additive enhancement of GPP (+17% relative to the temperature alone) and R (+11% relative to temperature
423 alone) but countered the effect on GPP/R and G_{net} (no significant difference from the control). Given the effect
424 of each of these treatments (T and OM) independently on sediment GPP/R and G_{net}, and the significant positive
425 correlation between G_{net} and GPP/R, this result is not surprising. A decrease in GPP/R and G_{net} due to warming
426 was countered by an increase in GPP/R and G_{net} due to an increased concentration of OM.

427 This finding raises questions within the context of each treatment, as mean SST on coral reefs will continuously
428 rise from now until beyond 2100, consistently affecting sediment metabolism. However, organic matter
429 enrichment of permeable coral reef carbonate sediments is also likely to gradually increase due to enhanced
430 algal production from elevated nutrients (Furnas et al., 2005), enhanced mucus production due to enhanced
431 terrestrial sedimentation (Alongi and McKinnon, 2005) and elevated terrestrial input of OM (Diaz-Ortega and
432 Hernandez-Delgado, 2014). As discussed above this long-term enrichment with OM will most likely make coral
433 reef sediments more heterotrophic (and not more autotrophic as in this short-term study). However the
434 subsequent response in G_{net} over longer timescales is less clear, as some work has shown that the degradation of
435 organic matter can enhance sediment dissolution (Andersson, 2015) whereas other work (e.g., Yeakel et al.,
436 2015) has shown that community calcification may actually increase. Therefore, combined with an increase in
437 T, the effect of long-term enrichment of OM on GPP/R is likely to be additive (decrease GPP/R), but the long-
438 term response in G_{net} still needs to further examination.

439 Similarly, the effect of other, more persistent products of eutrophication, namely dissolved inorganic nutrients
440 (DIN: NH_4^+, NO_3^-, PO_4^{3-}), on coral reef sediment GPP/R and G_{net} have yet to be studied and may become more

Biogeosciences Discuss., doi:10.5194/bg-2017-109, 2017
Manuscript under review for journal Biogeosciences
Discussion started: 28 April 2017

frequent and persistent as coastal land use changes continue to facilitate the increased runoff of fertilizers (Koop et al., 2001). Consequently, the results presented here provide an estimation of the future short-term response in coral reef sediment GPP/R and G_{net} to select forms of global warming (+2.4 ºC) and eutrophication (PD and CM), but by no means have explored other potential warming- and eutrophication-mediated perturbations that continue to threaten coral reef ecosystems. Future work should consider varying frequencies (e.g., > 24 hours) and forms of eutrophication (e.g., DIN) as well as a range of T, both within and beyond reported optimal ranges (> 2.4 ºC), to better constrain our understanding of the potential feedback responses in coral reef sediment GPP/R and G_{net}.

4.4 Conclusions

Overall**,** the results of this study suggest that seawater warming will shift GPP/R and G_{net} in permeable calcium carbonate coral reef sediments to a state of net heterotrophy and net dissolution, respectively, by the year 2100. Alternatively, short-term eutrophication, and the subsequent production of OM in the form of phytodetritus and coral mucus, could enhance sediment GPP/R and G_{net}. The combined effect of seawater warming and increased concentrations of OM may additively enhance sediment GPP and R, but the net effect on GPP/R and G_{net} will likely counter one another on relatively short timescales (22 hours). The future response in the net-flux-behaviour of CO_2 and O_2 in the coral reef sediment environment, and the consequent rate of carbon sequestration into the sediments, will likely depend on the relative frequency of each perturbation. The effects of OM (e.g., phytoplankton growth, reef-wide mucus secretion) on sediment metabolism generally persist temporarily (days to weeks) relative to global warming, a constant process which will continue to occur throughout this century and beyond. Provided this ecological context and the findings from this study, we propose that increased concentrations of OM, in the form of phytodetritus and coral mucus, will increase G_{net} and GPP/R in the sediment on relatively short timescales. However, once seawater temperature on coral reefs rises 2.4 ºC above the present day mean, the immediate effect of OM on sediment metabolism will be compromised by a warming-mediated net decrease in G_{net} and GPP/R, thereby limiting the ability of permeable calcium carbonate sediments on coral reefs to accumulate calcium carbonate.

Acknowledgements

We would like to thank Jacob Yeo for his assistance in the field. This research was funded by ARC Discovery Grant DP150102092.

Biogeosciences Discuss., doi:10.5194/bg-2017-109, 2017
Manuscript under review for journal Biogeosciences
Discussion started: 28 April 2017

References

Alongi, D. M. and McKinnon, A. D.: The cycling and fate of terrestrially-derived sediments and nutrients in the coastal zone of the Great Barrier Reef shelf, in Marine Pollution Bulletin, vol. 51, pp. 239–252., 2005.

Andersson, A. J.: A fundamental paradigm for coral reef carbonate sediment dissolution, Front. Mar. Sci., 2, 52, doi:10.3389/fmars.2015.00052, 2015.

Atkinson, M. J.: Biogeochemistry of nutrients, in Coral Reefs: An Ecosystem in Transition, pp. 199–206, Springer Netherlands, Dordrecht., 2011.

Bahr, K. D., Jokiel, P. L. and Rodgers, K. S.: Influence of solar irradiance on underwater temperature recorded by temperature loggers on coral reefs, Limnol. Oceanogr. Methods, 14(5), n/a-n/a, doi:10.1002/lom3.10093, 2016.

Bell, P. R. F.: Eutrophication and coral reefs-some examples in the Great Barrier Reef lagoon, Water Res., 26(5), 553–568, doi:10.1016/0043-1354(92)90228-V, 1992.

Bernacchi, C. J., Singsaas, E. L., Pimentel, C., Portis, a. R. R. and Long, S. P.: Improved temperature response functions for models of Rubisco-limited photosynthesis, Plant, Cell Environ., 24(2), 253–259, doi:10.1046/j.1365-3040.2001.00668.x, 2001.

Chanson, M. and Millero, F. J.: Effect of filtration on the total alkalinity of open-ocean seawater, Limnol. Oceanogr. Methods, 5, 293–295, doi:10.4319/lom.2007.5.293, 2007.

Cyronak, T., Santos, I. R. and Eyre, B. D.: Permeable coral reef sediment dissolution driven by elevated pCO2 and pore water advection, Geophys. Res. Lett., 40(18), 4876–4881, doi:10.1002/grl.50948, 2013.

Cyronak, T., Santos, I. R., McMahon, A. and Eyre, B. D.: Carbon cycling hysteresis in permeable carbonate sands over a diel cycle: Implications for ocean acidification, Limnol. Oceanogr., 58(1), 131–143, doi:10.4319/lo.2013.58.1.0131, 2013.

Cyronak, T. and Eyre, B. D.: The synergistic effects of ocean acidification and organic metabolism on calcium carbonate (CaCO3) dissolution in coral reef sediments, Mar. Chem., 183, 1–12, doi:10.1016/j.marchem.2016.05.001, 2016.

Díaz-ortega, G. and Hernández-Delgado, E. a: Unsustainable Land-Based Source Pollution in a Climate of Change: A Roadblock to the Conservation and Recovery of Elkhorn Coral Acropora palmata (Lamarck 1816), Nat. Resour., 5(10), 561–581, doi:10.4236/nr.2014.510050, 2014.

Dickson, A. G. and Millero, F. J.: A comparison of the equilibrium constants for the dissociation of carbonic acid in seawater media, Deep Sea Res. Part A. Oceanogr. Res. Pap., 34(10), 1733–1743, doi:10.1016/0198-0149(87)90021-5, 1987.

Dickson, A. G., Sabine, C. L. and Christian, J. R.: Guide to best practices for ocean CO2 measurements, North Pacific Marine Science Organization., 2007.

Ducklow, H. W. and Mitchell, R.: Composition of mucus released by coral reef coelenterates, Limnol. Oceanogr., 24(4), 706–714, doi:10.4319/lo.1979.24.4.0706, 1979.

Edinger, E. N., Jompa, J., Limmon, G. V, Widjatmoko, W. and Risk, M. J.: Reef degradation and coral biodiversity in Indonesia: Effects of land-based pollution, destructive fishing practices and changes over time, Mar. Pollut. Bull., 36(8), 617–630, doi:10.1016/S0025-326X(98)00047-2, 1998.

Eyre, B. D., Glud, R. N. and Patten, N.: Mass coral spawning: A natural large-scale nutrient addition experiment, Limnol. Oceanogr., 53(3), 997–1013, doi:10.4319/lo.2008.53.3.0997, 2008.

Biogeosciences Discuss., doi:10.5194/bg-2017-109, 2017
Manuscript under review for journal Biogeosciences
Discussion started: 28 April 2017

510 Eyre, B. D., Ferguson, A. J. P., Webb, A., Maher, D. and Oakes, J. M.: Metabolism of different benthic habitats
511 and their contribution to the carbon budget of a shallow oligotrophic sub-tropical coastal system (southern
512 Moreton Bay, Australia), Biogeochemistry, 102(1), 87–110, doi:10.1007/s10533-010-9424-7, 2011.

513 Eyre, B. D., Santos, I. R. and Maher, D. T.: Seasonal, daily and diel N2 effluxes in permeable carbonate
514 sediments, Biogeosciences, 10(4), 2601–2615, doi:10.5194/bg-10-2601-2013, 2013

515 Eyre, B. D., Andersson, A. J. and Cyronak, T.: Benthic coral reef calcium carbonate dissolution in an acidifying
516 ocean, Nat. Clim. Chang., 4(11), 969–976, doi:10.1038/nclimate2380, 2014.

517 Eyre, B. D., Oakes, J. M. and Middelburg, J. J.: Fate of microphytobenthos nitrogen in subtropical subtidal
518 sediments: A 15N pulse-chase study, Limnol. Oceanogr., 61(6), 2108–2121, doi:10.1002/lno.10356, 2016.

519 Fabricius, K. E.: Effects of terrestrial runoff on the ecology of corals and coral reefs: Review and synthesis,
520 Mar. Pollut. Bull., 50(2), 125–146, doi:10.1016/j.marpolbul.2004.11.028, 2005.

521 Ferguson, A., Eyre, B. and Gay, J.: Organic matter and benthic metabolism in euphotic sediments along shallow
522 sub-tropical estuaries, northern New South Wales, Australia, Aquat. Microb. Ecol., 33(2), 137–154,
523 doi:10.3354/ame033137, 2003.

524 Ferrier-Pagès, C., Leclercq, N., Jaubert, J. and Pelegrí, S. P.: Enhancement of pico- and nanoplankton growth by
525 coral exudates, Aquat. Microb. Ecol., 21(2), 203–209, doi:10.3354/ame021203, 2000.

526 Furnas, M., Mitchell, A., Skuza, M. and Brodie, J.: In the other 90%: Phytoplankton responses to enhanced
527 nutrient availability in the Great Barrier Reef Lagoon, in Marine Pollution Bulletin, vol. 51, pp. 253–265.,
528 2005.

529 Glud, R. N., Eyre, B. D. and Patten, N.: Biogeochemical responses to mass coral spawning at the Great Barrier
530 Reef: Effects on respiration and primary production, Limnol. Oceanogr., 53(3), 1014–1024,
531 doi:10.4319/lo.2008.53.3.1014, 2008.

532 Grigg, R. W.: Coral reefs in an urban embayment in Hawaii: a complex case history controlled by natural and
533 anthropogenic stress, Coral Reefs, 14(4), 253–266, doi:10.1007/BF00334349, 1995.

534 Guillard, R. R. L.: Culture of Phytoplankton for Feeding Marine Invertebrates, in Culture of Marine Invertebrate
535 Animals, pp. 29–60, Springer US, Boston, MA., 1975.

536 Hancke, K. and Glud, R. N.: Temperature effects on respiration and photosynthesis in three diatom-dominated
537 benthic communities, Aquat. Microb. Ecol., 37(3), 265–281, doi:10.3354/ame037265, 2004.

538 Hancke, K., Sorrell, B. K., Chresten Lund-Hansen, L., Larsen, M., Hancke, T. and Glud, R. N.: Effects of
539 temperature and irradiance on a benthic microalgae community: A combined two-dimensional oxygen and
540 fluorescence imaging approach, Limnol. Oceanogr., 59(5), 1599–1611, doi:10.4319/lo.2014.59.5.1599,
541 2014.

542 Huettel, M. and Gust, G.: Solute release mechanisms from confined sediment cores in stirred benthic chambers
543 and flume flows, Mar. Ecol. Prog. Ser., 82, 187–197, doi:10.3354/meps082187, 1992.

544 IPCC Summary for policymakers. Climate Change 2013: The Physical Science Basis Contribution of Working
545 Group I to the Fifth Assessment Report of the Intergovernmental Panel on Climate Change. Cambridge
546 University Press, Cambridge, United Kingdom and New York, NY USA. 2013

547 Johnson, M. D. and Carpenter, R. C.: Ocean acidification and warming decrease calcification in the crustose
548 coralline alga Hydrolithon onkodes and increase susceptibility to grazing, J. Exp. Mar. Bio. Ecol., 434–435,
549 94–101, doi:10.1016/j.jembe.2012.08.005, 2012.

Biogeosciences Discuss., doi:10.5194/bg-2017-109, 2017
Manuscript under review for journal Biogeosciences
Discussion started: 28 April 2017

550 Koop, K., Booth, D., Broadbent, A., Brodie, J., Bucher, D., Capone, D., Coll, J., Dennison, W., Erdmann, M.,
551 Harrison, P., Hoegh-Guldberg, O., Hutchings, P., Jones, G. B., Larkum, A. W. D., O'Neil, J., Steven, A.,
552 Tentori, E., Ward, S., Williamson, J. and Yellowlees, D.: ENCORE: The effect of nutrient enrichment on
553 coral reefs. Synthesis of results and conclusions, Mar. Pollut. Bull., 42(2), 91–120, doi:10.1016/S0025-
554 326X(00)00181-8, 2001.

555 Lavigne, H. and Gattuso, J.P.:Package 'seacarb': seawater carbonate chemistry with R, v. 2.4. 8 (ed. R
556 Development Core Team). See http.cran.r-project.org/web/ packages/seacarb/index.html, 2013.

557 Levitus, S., Antonov, J. I., Boyer, T. P. and Stephens, C.: Warming of the World Ocean, Science (80-.).,
558 287(March), 2225–2229, doi:10.1126/science.287.5461.2225, 2000.

559 López-Urrutia, Á. and Morán, X. A. G.: Resource limitation of bacterial production distorts the temperature
560 dependence of oceanic carbon cycling, Ecology, 88(4), 817–822, doi:10.1890/06-1641, 2007.

561 Maher, D. T., Santos, I. R., Leuven, J. R. F. W., Oakes, J. M., Erler, D. V., Carvalho, M. C. and Eyre, B. D.:
562 Novel Use of Cavity Ring-down Spectroscopy to Investigate Aquatic Carbon Cycling from Microbial to
563 Ecosystem Scales, Environ. Sci. Technol., 47(22), 12938–12945, doi:10.1021/es4027776, 2013.

564 Mallela, J. and Perry, C. T.: Calcium carbonate budgets for two coral reefs affected by different terrestrial runoff
565 regimes, Rio Bueno, Jamaica, Coral Reefs, 26(1), 129–145, doi:10.1007/s00338-006-0169-7, 2007.

566 Mehrbach, C. and Carl: Measurement of the apparent dissociation constants of carbonic acid in seawater at
567 atmospheric pressure, 1973.

568 Middelburg, J. J., Soetaert, K. and Herman, P. M. J.: Empirical relationships for use in global diagenetic models,
569 Deep Sea Res. Part I Oceanogr. Res. Pap., 44(2), 327–344, doi:10.1016/S0967-0637(96)00101-X, 1997.

570 Moriarty, D. J. W., Pollard, P. C. and Hunt, W. G.: Temporal and spatial variation in bacterial production in the
571 water column over a coral reef, Mar. Biol., 85(3), 285–292, doi:10.1007/BF00393249, 1985.

572 Odum, H. T. and Odum, E. P.: Trophic Structure and Productivity of a Windward Coral Reef Community on
573 Eniwetok Atoll, Ecol. Monogr., 25(3), 291–320, doi:10.2307/1943285, 1955.

574 Orlando, J. L. and Yee, S. H.: Linking Terrigenous Sediment Delivery to Declines in Coral Reef Ecosystem
575 Services, Estuaries and Coasts, 40(2), 359–375, doi:10.1007/s12237-016-0167-0, 2017.

576 Pandolfi, J. M., Connolly, S. R., Marshall, D. J. and Cohen, A. L.: Projecting coral reef futures under global
577 warming and ocean acidification., Science (80-)., 333(6041), 418–422, doi:10.1126/science.1204794, 2011.

578 Rabalais, N. N., Turner, R. E., Díaz, R. J. and Justić, D.: Global change and eutrophication of coastal waters,
579 ICES J. Mar. Sci., 66(7), 1528–1537, doi:10.1093/icesjms/fsp047, 2009.

580 Rabouille, C., Mackenzie, F. T. and Ver, L. M.: Influence of the human perturbation on carbon, nitrogen, and
581 oxygen biogeochemical cycles in the global coastal ocean, Geochim. Cosmochim. Acta, 65(21), 3615–3641,
582 doi:10.1016/S0016-7037(01)00760-8, 2001.

583 Robinson, C.: Plankton gross production and respiration in the shallow water hydrothermal systems of Miles,
584 Aegean Sea, J. Plankton Res., 22(5), 887–906, doi:10.1093/plankt/22.5.887, 2000.

585 Roelfsema, R. T. C. M. and Roelfsema, R. T. C. M.: Spatial distribution of benthic microalgae on coral reefs
586 determined by remote sensing, Coral Reefs, 21(3), 264–274, doi:10.1007/s00338-002-0242-9, 2002.

587 Salmond, J, Loder, J, Roelfsema, C, Host, R, Passenger, J.: 2015 Heron Reef Health Report, Brisbane., 2015.

Biogeosciences Discuss., doi:10.5194/bg-2017-109, 2017
Manuscript under review for journal Biogeosciences
Discussion started: 28 April 2017

588 Shaw, E. C., Carpenter, R. C., Lantz, C. A. and Edmunds, P. J.: Intraspecific variability in the response to ocean
589 warming and acidification in the scleractinian coral Acropora pulchra, Mar. Biol., 163(10), 210,
590 doi:10.1007/s00227-016-2986-8, 2016.

591 SPSS Inc. IBM Corp. IBM SPSS Statistics for Windows, Version 22.0. Armonk, NY: IBM Corp, 2013.

592 Tait, L. W. and Schiel, D. R.: Impacts of Temperature on Primary Productivity and Respiration in Naturally
593 Structured Macroalgal Assemblages, edited by T. Crowe, PLoS One, 8(9), e74413,
594 doi:10.1371/journal.pone.0074413, 2013.

595 Trnovsky, D., Stoltenberg, L., Cyronak, T. and Eyre, B.D.: Antagonistic Effects of Ocean Acidification and
596 Rising Sea Surface Temperature on the Dissolution of Coral Reef Carbonate Sediments. Front in Mar Sci 3,
597 211, doi:10.3389/fmars.2016.00211, 2016.

598 Weston, N. B. and Joye, S. B.: Temperature-driven decoupling of key phases of organic matter degradation in
599 marine sediments, Proc. Natl. Acad. Sci. U. S. A., 102(47), 17036–17040, doi:10.1073/pnas.0508798102,
600 2005.

601 Wiencke, C., Rahmel, J., Karsten, U., Weykam, G. and Kirst, G. O.: Photosynthesis of marine macroalgae from
602 Antarctica: Light and temperature requirements, Bot Act, 106(1), 78–87, doi:10.1111/j.1438-
603 8677.1993.tb00341.x, 1993.

604 Wild, C., Huettel, M., Klueter, A., Kremb, S. G., Rasheed, M. Y. M. and Jørgensen, B. B.: Coral mucus
605 functions as an energy carrier and particle trap in the reef ecosystem., Nature, 428(6978), 66–70,
606 doi:10.1038/nature02344, 2004.

607 Wild, C., Rasheed, M., Werner, U., Franke, U., Johnstone, R. and Huettel, M.: Degradation and mineralization
608 of coral mucus in reef environments, Mar. Ecol. Prog. Ser., 267, 159–171, doi:10.3354/meps267159, 2004.

609 Wild, C., Rasheed, M., Jantzen, C., Cook, P., Struck, U., Huettel, M. and Boetius, A.: Benthic metabolism and
610 degradation of natural particulate organic matter in carbonate and silicate reef sands of the northern Red Sea,
611 Mar. Ecol. Prog. Ser., 298, 69–78, doi:10.3354/meps298069, 2005.

612 Wilkinson, C. R.: Microbial ecology on a coral reef, Search, 18, 31–33, 1987.Woodwell, G. M., Mackenzie, F.
613 T., Houghton, R. A., Apps, M., Gorham, E. and Davidson, E.: Biotic feedbacks in the warming of the earth,
614 Clim. Change, 40(3/4), 495–518, doi:10.1023/A:1005345429236, 1998.

615 Yvon-Durocher, G., Jones, J. I., Trimmer, M., Woodward, G. and Montoya, J. M.: Warming alters the metabolic
616 balance of ecosystems, Philos. Trans. R. Soc. B Biol. Sci., 365(1549), 2117–2126,
617 doi:10.1098/rstb.2010.0038, 2010.

Biogeosciences Discuss., doi:10.5194/bg-2017-109, 2017
Manuscript under review for journal Biogeosciences
Discussion started: 28 April 2017

618 **Tables**

Table 1: Concentrations of carbon (µmol C L^{-1}) and nitrogen (µmol N L^{-1}) and measured temperature (ºC) in the control and treatment chambers. Values correspond to the mean ± SE. Control (C) (n = 9) and temperature (T) (n = 7) treatments were pooled together from all four incubations. Organic matter (OM) (phytodetritus (PD) and coral mucus (CM)) and combination treatments (T + PD, T + CM) are pooled together from the two incubations for that specific OM treatment (n = 4).

Treatment	Carbon (µmol C L^{-1})	Nitrogen (µmol N L^{-1})	Temperature (ºC)
C	0.63 ± 0.13	0.12 ± 0.08	28.2 ± 1.1
T	0.63 ± 0.13	0.12 ± 0.08	30.6 ± 1.0
PD	21.7 ± 1.0	2.3 ± 0.8	28.4 ± 1.0
T + PD	21.7 ± 1.0	2.3 ± 0.8	30.5 ± 0.9
CM	24.2 ± 1.1	1.5 ± 0.4	28.3 ± 0.8
T + CM	24.2 ± 1.1	1.5 ± 0.4	30.7 ± 1.1

Biogeosciences Discuss., doi:10.5194/bg-2017-109, 2017
Manuscript under review for journal Biogeosciences
Discussion started: 28 April 2017

Table 2: The equations used in this study to calculate rates of sediment metabolism based on measured fluxes in dissolved oxygen (DO) and total alkalinity (A_T) (Eyre et al. (2011).

Metabolic Rate	Definition
Respiration (R)	Dark DO Flux x -1
Net Primary Production (NPP)	Light DO Flux
Gross Primary Production (GPP)	NPP + R
GPP/R	GPP x 12 (daylight hours)/ R x 24 (total hours)
Net Calcification (G_{net})	A_T Flux x 0.5; positive values represent net calcification and negative rates represent net dissolution

Biogeosciences Discuss., doi:10.5194/bg-2017-109, 2017
Manuscript under review for journal Biogeosciences
Discussion started: 28 April 2017

Table 3: Calculated gross primary productivity (GPP: mmol O_2 m^{-2} hr^{-1}) respiration (R: mmol O_2 m^{-2} hr^{-1}), the ratio of GPP/R, and net calcification (G_{net}: mmol $CaCO_3$ m^{-2} hr^{-1}) in the control and treatment chambers. Values correspond to the mean ± SE. Control (C) (n = 9) and temperature (T) (n = 7) treatments were pooled together from all four incubations. OM treatments (phytodetritus (PD) and coral mucus (CM)) and combination treatments (T + PD, T + CM) are pooled together from the two incubations for that specific OM source (n = 4).

Treatment	R (mmol O_2 m^{-2} hr^{-1})	GPP (mmol O_2 m^{-2} hr^{-1})	GPP/R	G_{net} (mmol $CaCO_3$ m^{-2} hr^{-1})
C	- 1.3 ± 0.5	3.2 ± 0.6	1.31 ± 0.1	0.2 ± 0.2
T	- 3.5 ± 0.4	6.4 ± 0.5	0.91 ± 0.1	- 0.1 ± 0.1
PD	- 2.6 ± 0.5	7.9 ± 0.4	1.54 ± 0.1	0.6 ± 0.2
T + PD	- 3.1 ± 0.5	7.8 ± 0.5	1.27 ± 0.1	0.3 ± 0.1
CM	- 2.0 ± 0.4	6.4 ± 0.7	1.61 ± 0.2	0.5 ± 0.2
T + CM	- 2.9 ± 0.4	7.4 ± 0.5	1.25 ± 0.1	0.2 ± 0.2

Biogeosciences Discuss., doi:10.5194/bg-2017-109, 2017
Manuscript under review for journal Biogeosciences
Discussion started: 28 April 2017

619 **Figures**

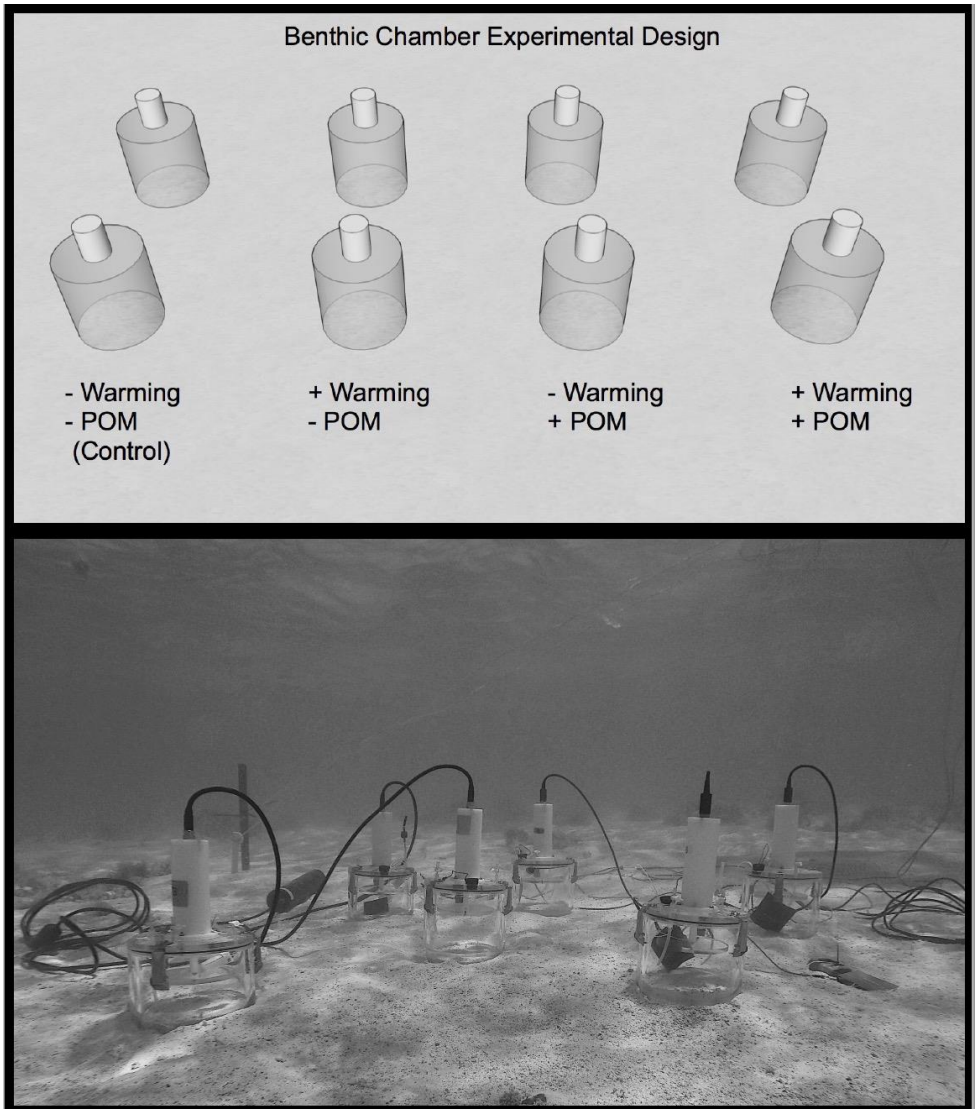

620

621 **Figure 1:** Layout of the experimental design using benthic chambers. Eight chambers were used in total, which
622 provided two replicates per treatment. Chambers are organized by the presence (+) and absence (-) of the
623 warming (+2.4 ºC) and organic matter (OM) (phytodetritus or coral mucus) treatments.

Biogeosciences Discuss., doi:10.5194/bg-2017-109, 2017
Manuscript under review for journal Biogeosciences
Discussion started: 28 April 2017

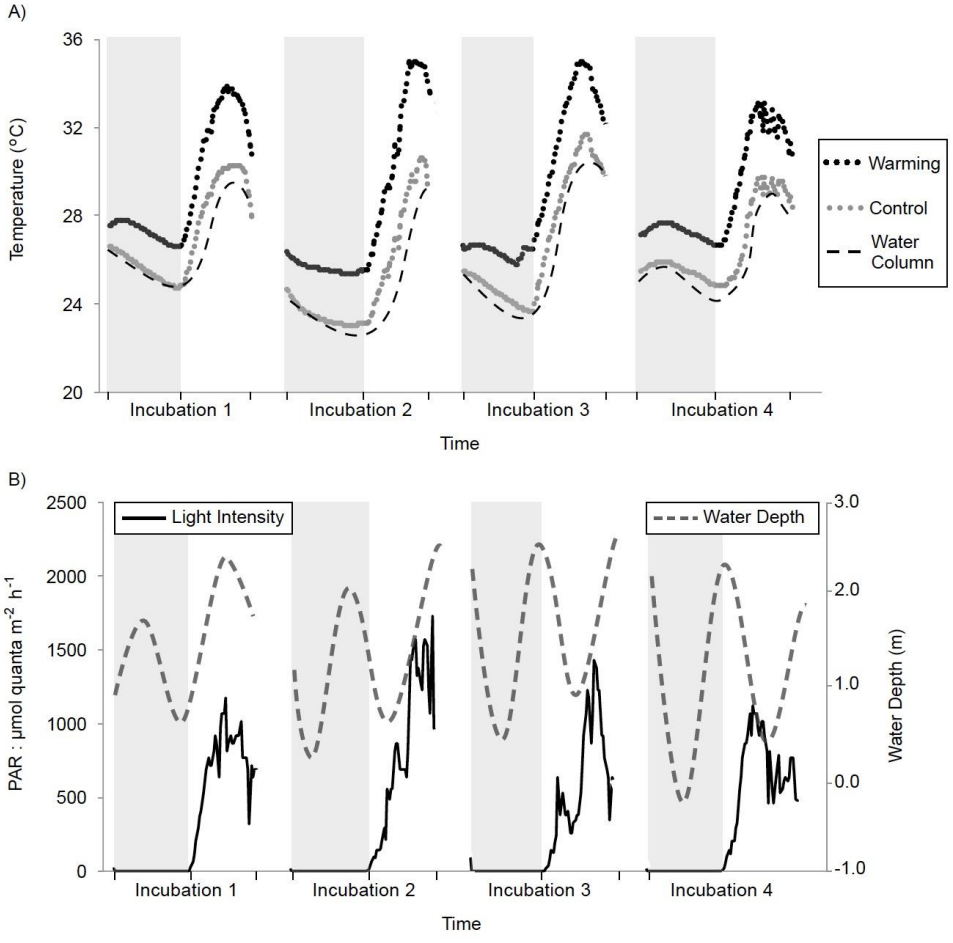

Figure 2: Water column parameters measured during the four incubations, each starting at sunset (18:00) and ending at the following day's dusk (16:00). Data are presented from the first phase (Incubation 1 and 2) where phytodetritus was used as an organic matter (OM) treatment, and from the second phase (Incubation 3 and 4), where coral mucus was used as an OM treatment. Shaded grey bars represent night time. A) Mean temperature (°C) measured by Hobo temperature recorders that logged temperature at fifteen-minute intervals during each incubation period. Data are pooled together as the mean from control (grey dots) and warming (black dots) treatments (n = 4 per incubation). Mean water column temperature (n = 1 per incubation) shown as a black dash. B) Measured light intensity (µmol quanta m^{-2} s^{-1}) in the water column (black line) and water height (m) during each incubation period (grey dash).

Biogeosciences Discuss., doi:10.5194/bg-2017-109, 2017
Manuscript under review for journal Biogeosciences
Discussion started: 28 April 2017

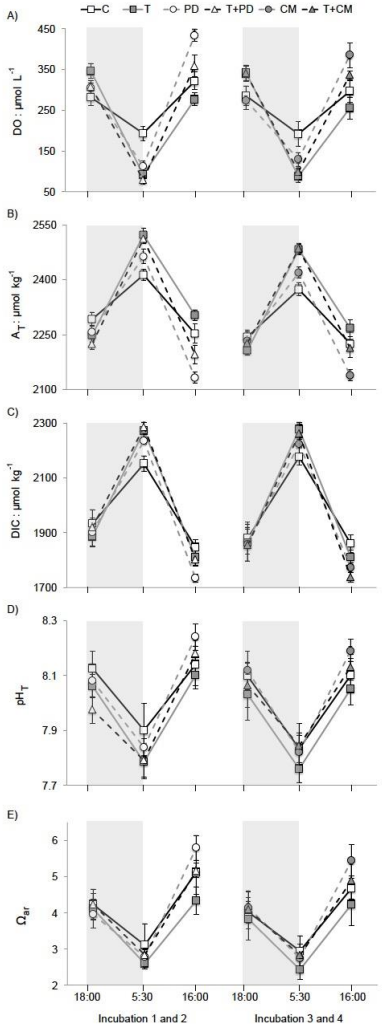

634

635 **Figure 3:** Water chemistry (mean ± SE) measured and calculated during the four incubations. Control (C),
636 warming (T), phytodetritus (PD), coral mucus (CM), and combination (T + PD, T + CM) treatments are
637 averaged over the two incubations (and replicate chambers therein) in which each respective OM treatment was
638 used (n = 4). Shaded grey bars represent the dark and time of sampling is labelled on the x-axis. A) Measured
639 fluxes in dissolved oxygen (DO: µmol L^{-1}). B) Measured fluxes in total alkalinity (A_T: µmol kg^{-1}). C) Measured
640 fluxes in dissolved inorganic carbon (DIC: µmol kg^{-1}). D) Calculated changes in pH (total scale: pH_T). E)
641 Calculated fluxes in aragonite saturation state (Ω_{ar}).

Biogeosciences Discuss., doi:10.5194/bg-2017-109, 2017
Manuscript under review for journal Biogeosciences
Discussion started: 28 April 2017

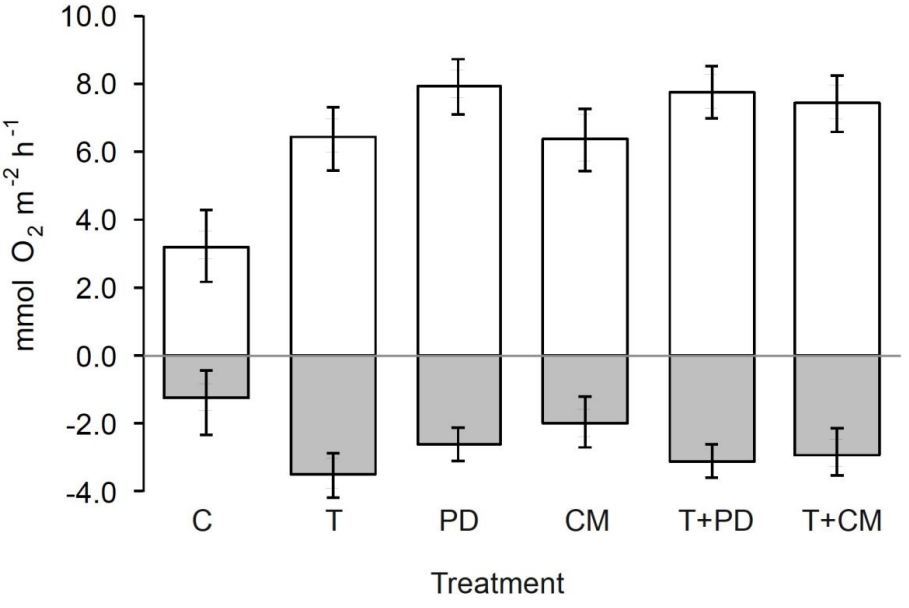

642

643 **Figure 4:** Mean sediment gross primary production (GPP: mmol O_2 m^{-2} h^{-1}) and respiration (R: mmol O_2 m^{-2} h^{-1}) in response to warming (+2.4 ºC) and each OM treatment (phytodetritus and coral mucus). Control (C) (n = 9) and warming (T) (n = 7) treatments are averaged over all four incubations and the replicate chambers therein. Phytodetritus (PD), coral mucus (CM), and combination (T + PD, T + CM) treatments are averaged over the two incubations (and replicate chambers therein) in which each respective OM treatment was used (n = 4). Average measured rates ± SE are represented in white for GPP (positive) and grey for R (negative).

Biogeosciences Discuss., doi:10.5194/bg-2017-109, 2017
Manuscript under review for journal Biogeosciences
Discussion started: 28 April 2017

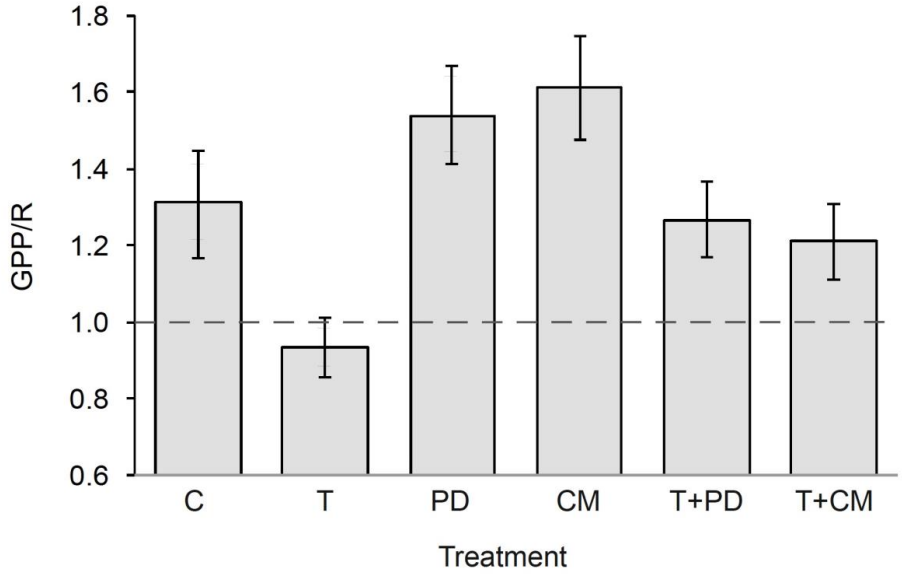

649

650 **Figure 5:** Mean ± SE sediment gross primary production (12 hour) to respiration (24 hour) ratios (GPP/R) in
651 response to warming (+2.4 ºC) and each OM treatment (phytodetritus and coral mucus). Control (C) (n = 9) and
652 warming (T) (n = 7) treatments are averaged over all four incubations and the replicate chambers therein, while
653 phytodetritus (PD), coral mucus (CM), and combination (T + PD, T + CM) treatments are averaged over the two
654 incubations (and replicate chambers therein) in which each respective OM treatment was used (n = 4). Dashed
655 grey line represents the divide between net heterotrophy and net autotrophy (GPP/R = 1).

Biogeosciences Discuss., doi:10.5194/bg-2017-109, 2017
Manuscript under review for journal Biogeosciences
Discussion started: 28 April 2017

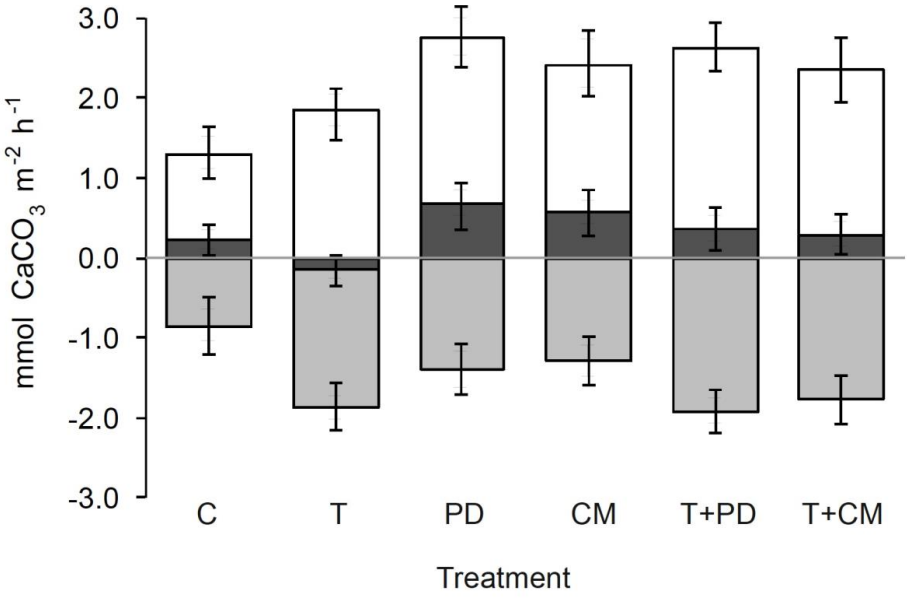

656

657 **Figure 6:** Mean sediment net calcification (G_{net}: mmol $CaCO_3$ m^{-2} h^{-1}) in response to warming (+2.4 ºC) and
658 each OM treatment (phytodetritus and coral mucus). Control (C) (n = 9) and warming (T) (n = 7) treatments are
659 averaged over all four incubations and the replicate chambers therein, while phytodetritus (PD), coral mucus
660 (CM), and combination (T + PD, T + CM) treatments are averaged over the two incubations (and replicate
661 chambers therein) in which each respective OM treatment was used (n = 4). Average measured rates ± SE are
662 represented in white for light G_{net} (positive) and grey for dark G_{net} (negative). Black bars represent the 24-hour
663 diel G_{net} averaged from light and dark measurements.

Biogeosciences Discuss., doi:10.5194/bg-2017-109, 2017
Manuscript under review for journal Biogeosciences
Discussion started: 28 April 2017

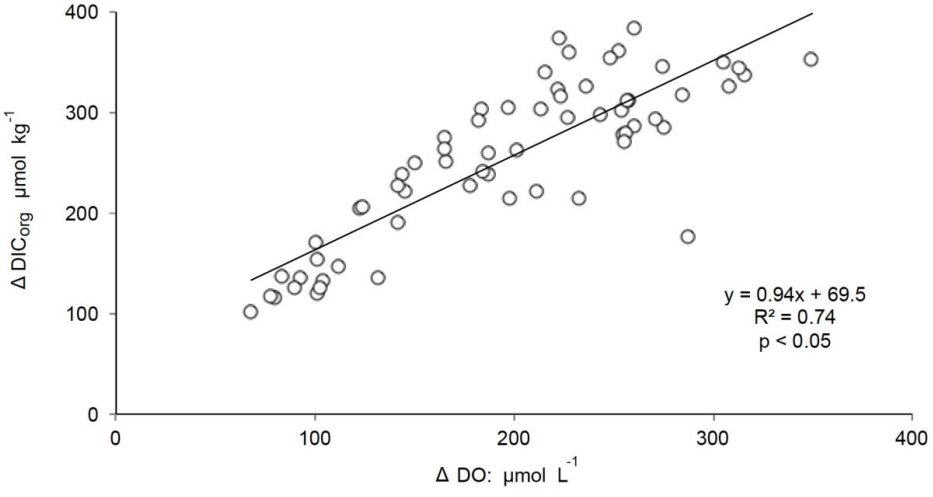

664

665 **Figure 7:** A linear correlation between calculated changes in dissolved inorganic carbon (ΔDIC_{org}: µmol kg^{-1}) as
666 a function of measured changes in dissolved oxygen (ΔDO: µmol L^{-1}) over each 12-hour sampling period from
667 all chambers and incubations. To examine the variation in DIC due solely to photosynthesis and respiration
668 (DIC_{org}), changes in DIC were corrected for calcium carbonate precipitation/dissolution using the measured
669 changes in total alkalinity (A_T) (0.5 moles CO_2: 1 mole A_T).

Biogeosciences Discuss., doi:10.5194/bg-2017-109, 2017
Manuscript under review for journal Biogeosciences
Discussion started: 28 April 2017

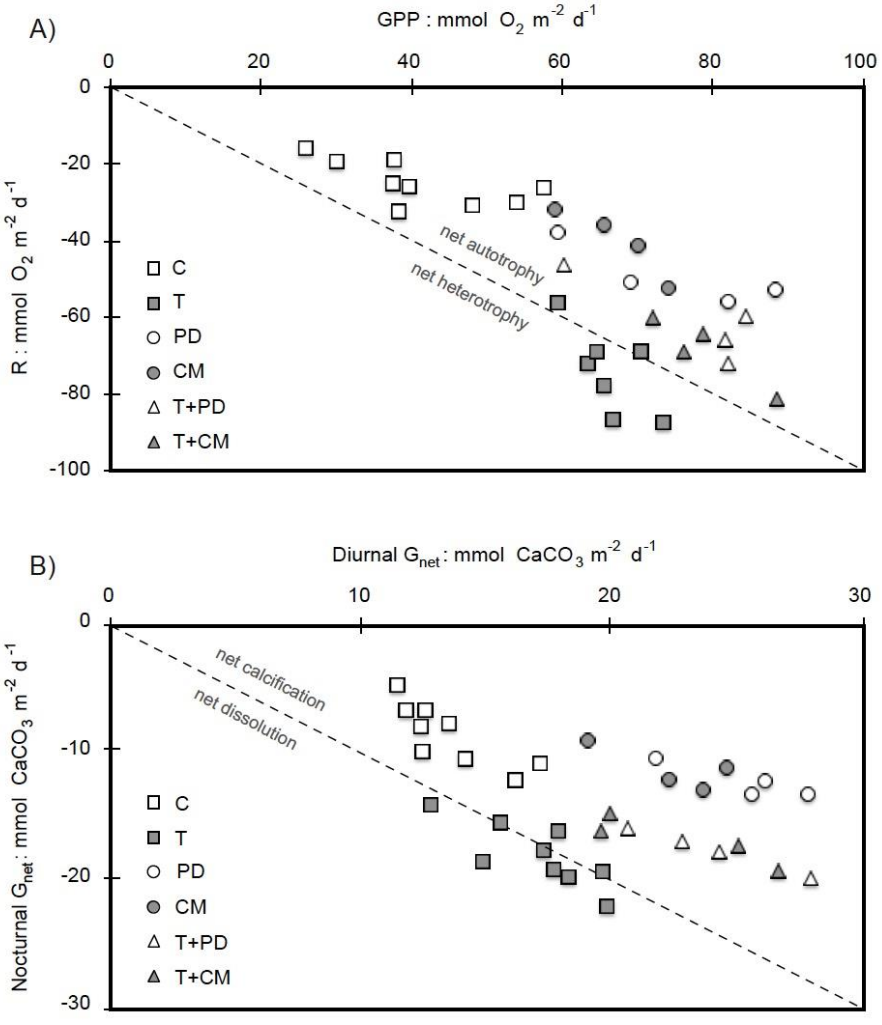

Figure 8: Measured metabolic rates from the control (C) (n = 9) and warming (T) (n = 7) treatments are displayed from all four incubations and the replicate chambers therein. Phytodetritus (PD), coral mucus (CM), and combination (T + PD, T + CM) treatments are displayed from the two incubations (and replicate chambers therein) where each respective OM treatment was used (n = 4). A) Respiration (R: mmol O_2 m^{-2} d^{-1}) plotted as a function of gross primary production (GPP: mmol O_2 m^{-2} d^{-1}). Dashed line represents the divide between net heterotrophy and net autotrophy (GPP/R = 1). B) Dark dissolution (Dark G: mmol $CaCO_3$ m^{-2} d^{-1}) plotted as a function of daytime calcification (Diurnal G: mmol $CaCO_3$ m^{-2} d^{-1}). Dashed line represents the divide between net calcification and net dissolution (G_{net} = 0).